AJNR

Diffusion-Weighted MR Imaging in Normal Human Brains in Various Age Groups

Johanna Helenius, Lauri Soinne, Jussi Perkiö, Oili Salonen, Aki Kangasmäki, Markku Kaste, Richard A. D. Carano, Hannu J Aronen and Turgut Tatlisumak

AJNR Am J Neuroradiol 2002, 23 (2) 194-199
http://www.ajnr.org/content/23/2/194

AJNR Am J Neuroradiol 23:194–199, February 2002

Diffusion-Weighted MR Imaging in Normal Human Brains in Various Age Groups

Johanna Helenius, Lauri Soinne, Jussi Perkiö, Oili Salonen, Aki Kangasmäki, Markku Kaste, Richard A. D. Carano, Hannu J Aronen, and Turgut Tatlisumak

BACKGROUND AND PURPOSE: **Few studies have concerned the absolute apparent diffusion coefficient (ADC) values in the normal human brain and the effect of aging on diffusion. Therefore, our purpose was to determine whether the average ADC (ADC_{av}) values in the various regions of the brain differ with age, sex, or hemisphere and to establish reference values of the absolute ADC_{av} for further studies.**

METHODS: **Subjects (40 men and 40 women) were chosen from a healthy population; age groups were 20–34, 35–49, and 50–64 years and 65 years or older (n = 20 each). All subjects were examined with MR imaging, including conventional and diffusion-weighted imaging in three orthogonal directions with two b values (0 and 1000 s/mm^2) at 1.5 T. Bilateral ADC_{av} values were determined in 36 regions of interest encompassing the entire brain.**

RESULTS: **ADC_{av} values were highest in the cortical gray matter ([0.89 ± 0.04] × 10^{-3} mm^2/s; range, 0.78–1.09 × 10^{-3}), lower in the deep gray matter ([0.75 ± 0.03] × 10^{-3} mm^2/s; range, 0.64–0.83 × 10^{-3}), and lowest in the white matter ([0.70 ± 0.03] × 10^{-3} mm^2/s; range, 0.62–0.79 × 10^{-3}). The ADC_{av} values did not significantly change with aging, except for an increase in the lateral ventricles. No difference was observed between women and men or between the hemispheres.**

CONCLUSION: **The data reported herein are representative, and the ADC_{av} values can be used for reference in future studies and in clinical settings.**

Diffusion-weighted (DW) MR imaging reveals ischemic regions in the brain within minutes after the induction of focal ischemia in experimental stroke (1, 2) and as soon as a patient with acute stroke is available for imaging studies (3). DW imaging has become an essential part of the imaging examination of patients with hyperacute stroke (4). Recently, its utility has been investigated in several other brain diseases, including epilepsy (5), Alzheimer disease (6), multiple sclerosis (7, 8), and Parkinson disease (9). DW imaging is based on the random translational movement of water molecules in biologic media. The net diffusion of the molecules is referred to as the apparent diffusion coefficient (ADC) (10). Because the cellular structures are distributed anisotropically, the measurement of diffusion is direction dependent (11); this fact emphasizes the need for measuring diffusion in several directions. Thus, to obtain a rotationally invariant estimate of the isotropic diffusion, DW images must be acquired in at least three orthogonal directions (12). Diffusion weighting is expressed with a b value, which is dependent on sequence characteristics. The b value increases with increasing diffusion weighting, and sufficient diffusion weighting is usually achieved with a b value of 1000 s/mm^2. The ADC value can be calculated as the slope of the natural logarithm of the signal intensity versus the b value. Two-point ADC estimates, with b = 0 and 1000 s/mm^2, are adequate for measuring diffusion in the human brain; they result in good agreement with six-point estimates of ADC (13, 14) and substantially shorten the imaging time.

Studies regarding absolute ADC values in the normal human brain and the effect of aging on diffusion are scarce, and only a few reports involving small numbers of subjects have been published (12, 15–18). Therefore, the purpose of this study was to determine whether the average ADC (ADC_{av}) values in the various regions of the brain differ with age, sex, or

Received December 19, 2000; accepted after revision September 26, 2001.

From the Departments of Neurology (J.H., L.S., M.K., T.T.) and Radiology (J.P., O.S., A.K., H.J.A.), Helsinki University Central Hospital, Finland; the Department of Physics (J.P., A.K.), University of Helsinki, Finland; and Synarc (R.A.D.C.), San Francisco, CA.

Supported in part by the Maire Taponen Foundation, the University of Helsinki, the Sigrid Juselius Foundation, and the Foundation of Neurology, Helsinki, Finland.

Address reprint requests to Dr Johanna Helenius, Department of Neurology, Helsinki University Central Hospital, Haartmaninkatu 4, 00290 Helsinki, Finland.

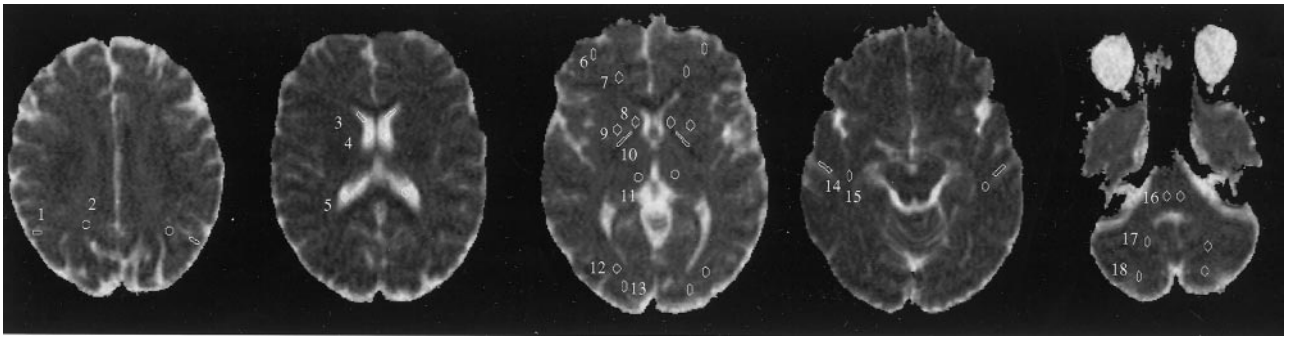

FIG 1. ROIs used in data analysis are superimposed on axial ADC_{av} maps. *1* indicates the parietal gray matter; *2*, parietal white matter; *3*, frontal horn of lateral ventricle; *4*, middle part of lateral ventricle; *5*, posterior horn of lateral ventricle; *6*, frontal gray matter; *7*, frontal white matter; *8*, caudate nucleus; *9*, putamen; *10*, internal capsule; *11*, thalamus; *12*, occipital white matter; *13*, occipital gray matter; *14*, temporal gray matter; *15*, temporal white matter; *16*, pons; *17*, cerebellar white matter; and *18*, cerebellar gray matter.

hemisphere (left or right) and to establish reference values of the absolute ADC_{av} for further studies.

Methods

Volunteer Characteristics

The present study was approved by the ethics committees of the Departments of Neurology and Radiology, Helsinki University Central Hospital, Finland, and it was performed according to the principles of the Declaration of Helsinki and institutional guidelines. All subjects provided written informed consent before their enrollment in the study. The study included 80 healthy volunteers chosen from a healthy population (40 men and 40 women), whose ages ranged from 22 to 85 years (men, 22–85 years; women, 22–82 years), with a mean age of 50.0 years ± 17.4 (men, 49.9 years ± 17.2; women, 50.1 years ± 17.9). Their age distribution was uniform within each of the four age groups (10 men and 10 women per group): group 1, 20–34 years (mean, 26.8 years ± 4.1; range, 22–34 years); group 2, 35–49 years (mean, 43.6 years ± 4.4; range, 36–49 years); group 3, 50–64 years (mean, 57.4 years ± 3.5; range, 52–64 years); and group 4, 65 years or older (mean, 72.2 years ± 5.2; range, 65–85 years).

A neurologist (L.S., T.T.) interviewed and examined the volunteers before imaging and excluded those for whom MR imaging was contraindicated (19). The volunteers had no symptoms, signs, or history of any neurologic or systemic disease that might have affected the brain (eg, diabetes, chronic obstructive pulmonary disease, hypertension, metabolic disorders), nor did they have a family history of dementia or multiple sclerosis. None was regularly taking medication, expect for female hormones for replacement therapy or topical drugs. Subjects in whom MR images revealed an unexpected cerebral lesion were excluded. All the subjects were white, and all except two were Finnish.

Imaging Techniques

All studies were performed with a Magnetom Vision imager (Siemens Medical Systems, Erlangen, Germany) operating at 1.5 T. A standard head coil with standard restraints was used to fix the volunteer's head position. In addition to axial DW images, conventional T1-weighted, T2-weighted, fluid-attenuated inversion recovery, and proton density–weighted images were obtained to exclude gross brain disease. Two physicians—first, a neurologist (L.S., T.T.) and, later, a neuroradiologist (O.S.)—independently evaluated the images as normal. Minor white matter changes (leukoaraiosis) in the older subjects were regarded as normal (20). All imaging studies were completed without any adverse effects or complications.

DW imaging was performed with a spin-echo echo-planar imaging sequence with a TR/TE of 4000/103, a gradient strength of 25 mT/m, 19 5-mm-thick sections, an intersection gap of 1.5 mm, a field of view of 230 × 230 mm^2, and a matrix size of 96 × 128 interpolated to 256 × 256. Diffusion was measured in three orthogonal directions (x, y, and z) with two b values (0 and 1000 s/mm^2). The total acquisition time for the DW images was 20 seconds.

Data Analysis

DW images were transferred to a separate workstation for data analysis. First, the images in the three orthogonal directions were coregistered. The natural logarithms of the images were averaged to form a rotationally invariant resultant image. By using a linear least-squares regression on a pixel-by-pixel basis, the resultant image and the natural logarithm of the reference T2-weighted image (b = 0) were fitted to the b values; the slope of the fitted line was the ADC_{av}. The calculations were performed with a commercially available software program (MatLab; Mathsoft, Natick, MA). In each hemisphere, 18 distinct neuroanatomic structures were selected for the analysis. These structures were the frontal, parietal, temporal, occipital, and cerebellar gray matter and white matter; the caudate nucleus; the putamen; the thalamus; the internal capsule; the pons; and the CSF in the lateral ventricles (frontal horn, middle part, posterior horn) (Fig 1). The regions of interest (ROIs) were manually drawn on the T2-weighted (b = 0) images on which the structures could easily be identified. They were subsequently transferred to the equivalent ADC_{av} maps. For each ROI, the surface area and the mean, SD, and range of the ADC_{av} values were obtained. The ROI analysis was performed with a commercially available image analysis software (Alice; Hayden Image Processing Group, Perceptive Systems, Boulder, CO).

Statistical Analysis

The regional variation and the effect of sex on the ADC_{av} values were studied by using the *t* test for dependent or independent samples, as appropriate. A one-way analysis of variance was applied to study the average values in the different regions of the brain. The groups representing different age cohorts and different sexes were compared with a multivariate analysis of variance. The homogeneity of the variances was studied with the Levene test. A two-tailed *P* value of less than .05 was considered to indicate a significant difference.

Results

In the whole brain, the mean ADC_{av} values were $(0.89 \pm 0.04) \times 10^{-3}$ mm^2/s (range, $0.78–1.09 \times 10^{-3}$

TABLE 1: ADC_{av} values in the 36 ROIs

ROI	ADC_{av} ($\times 10^{-3}$ mm²/s)						
	All (n = 80)	Men (n = 40)	Women (n = 40)	Age Group 1, 20–34 years (n = 20)	Age Group 2, 35–49 years (n = 20)	Age Group 3, 50–64 years (n = 20)	Age Group 4, 65–85 years (n = 20)
Gray matter							
Frontal left	0.89 ± 0.08 (0.72–1.18)	0.89 ± 0.08 (0.72–1.05)	0.89 ± 0.09 (0.72–1.18)	0.89 ± 0.06 (0.72–0.98)	0.88 ± 0.07 (0.72–1.00)	0.90 ± 0.12 (0.73–1.18)	0.88 ± 0.07 (0.80–1.00)
Frontal right	0.91 ± 0.08 (0.77–1.13)	0.90 ± 0.08 (0.77–1.11)	0.91 ± 0.08 (0.79–1.13)	0.92 ± 0.09 (0.80–1.13)	0.90 ± 0.10 (0.77–1.09)	0.90 ± 0.08 (0.80–1.13)	0.90 ± 0.06 (0.82–1.02)
Occipital left	0.90 ± 0.08 (0.67–1.09)	0.91 ± 0.07 (0.80–1.09)	0.90 ± 0.09 (0.67–1.09)	0.90 ± 0.09 (0.67–1.09)	0.90 ± 0.07 (0.78–1.08)	0.91 ± 0.09 (0.81–1.09)	0.90 ± 0.07 (0.80–1.02)
Occipital right	0.91 ± 0.11 (0.78–1.38)	0.90 ± 0.09 (0.78–1.07)	0.92 ± 0.13 (0.79–1.38)	0.91 ± 0.10 (0.80–1.13)	0.92 ± 0.10 (0.78–1.13)	0.93 ± 0.15 (0.78–1.38)	0.88 ± 0.08 (0.78–1.07)
Temporal left	0.88 ± 0.06 (0.66–1.01)	0.88 ± 0.05 (0.79–1.00)	0.87 ± 0.06 (0.66–1.01)	0.87 ± 0.05 (0.80–0.98)	0.89 ± 0.06 (0.79–1.01)	0.87 ± 0.07 (0.66–0.96)	0.87 ± 0.04 (0.80–0.97)
Temporal right	0.87 ± 0.09 (0.38–1.10)	0.88 ± 0.08 (0.75–1.10)	0.87 ± 0.10 (0.38–1.01)	0.87 ± 0.06 (0.79–1.04)	0.84 ± 0.13 (0.38–1.01)	0.87 ± 0.08 (0.80–1.10)	0.91 ± 0.70 (0.80–1.02)
Parietal left	0.89 ± 0.06 (0.75–1.10)	0.90 ± 0.06 (0.80–1.10)	0.89 ± 0.07 (0.75–1.07)	0.90 ± 0.05 (0.82–0.98)	0.88 ± 0.08 (0.75–1.10)	0.91 ± 0.06 (0.84–1.07)	0.89 ± 0.06 (0.80–1.04)
Parietal right	0.90 ± 0.08 (0.76–1.14)	0.91 ± 0.07 (0.79–1.08)	0.89 ± 0.09 (0.76–1.14)	0.90 ± 0.08 (0.76–1.06)	0.88 ± 0.09 (0.78–1.14)	0.92 ± 0.07 (0.78–1.08)	0.90 ± 0.08 (0.80–1.08)
Cerebellum left	0.84 ± 0.12 (0.65–1.13)	0.82 ± 0.13 (0.65–1.13)	0.85 ± 0.12 (0.66–1.08)	0.82 ± 0.12 (0.65–1.01)	0.82 ± 0.14 (0.65–1.13)	0.86 ± 0.11 (0.66–1.07)	0.84 ± 0.13 (0.65–1.08)
Cerebellum right	0.80 ± 0.14 (0.61–1.16)	0.78 ± 0.13 (0.65–1.16)	0.81 ± 0.14 (0.62–1.13)	0.79 ± 0.12 (0.64–1.08)	0.75 ± 0.13 (0.61–1.13)	0.83 ± 0.17 (0.64–1.16)	0.82 ± 0.12 (0.63–1.12)
White matter							
Frontal left	0.70 ± 0.07 (0.46–0.85)	0.69 ± 0.08 (0.46–0.85)	0.71 ± 0.07 (0.57–0.81)	0.68 ± 0.06 (0.56–0.78)	0.69 ± 0.08 (0.54–0.82)	0.71 ± 0.06 (0.59–0.81)	0.71 ± 0.09 (0.46–0.85)
Frontal right	0.71 ± 0.07 (0.54–0.90)	0.71 ± 0.08 (0.54–0.85)	0.71 ± 0.07 (0.54–0.90)	0.69 ± 0.08 (0.54–0.90)	0.72 ± 0.07 (0.57–0.83)	0.71 ± 0.06 (0.62–0.85)	0.71 ± 0.08 (0.54–0.85)
Occipital left	0.71 ± 0.04 (0.59–0.81)	0.70 ± 0.04 (0.63–0.78)	0.71 ± 0.05 (0.59–0.81)	0.71 ± 0.03 (0.64–0.78)	0.69 ± 0.05 (0.59–0.78)	0.70 ± 0.03 (0.63–0.75)	0.72 ± 0.05 (0.65–0.81)
Occipital right	0.71 ± 0.04 (0.59–0.82)	0.70 ± 0.03 (0.62–0.78)	0.71 ± 0.05 (0.59–0.82)	0.71 ± 0.04 (0.61–0.78)	0.69 ± 0.05 (0.59–0.77)	0.70 ± 0.03 (0.62–0.75)	0.72 ± 0.05 (0.66–0.82)
Temporal left	0.69 ± 0.06 (0.54–0.82)	0.68 ± 0.06 (0.54–0.79)	0.70 ± 0.06 (0.57–0.82)	0.69 ± 0.08 (0.57–0.80)	0.68 ± 0.06 (0.54–0.82)	0.68 ± 0.06 (0.58–0.80)	0.70 ± 0.05 (0.60–0.77)
Temporal right	0.69 ± 0.06 (0.50–0.80)	0.69 ± 0.06 (0.56–0.79)	0.69 ± 0.06 (0.50–0.80)	0.67 ± 0.06 (0.50–0.80)	0.69 ± 0.07 (0.58–0.80)	0.70 ± 0.06 (0.58–0.78)	0.69 ± 0.05 (0.56–0.79)
Parietal left	0.71 ± 0.04 (0.62–0.90)	0.71 ± 0.05 (0.62–0.90)	0.71 ± 0.04 (0.64–0.82)	0.70 ± 0.03 (0.63–0.76)	0.71 ± 0.05 (0.64–0.82)	0.69 ± 0.04 (0.62–0.77)	0.73 ± 0.05 (0.66–0.90)
Parietal right	0.71 ± 0.05 (0.63–0.90)	0.71 ± 0.05 (0.63–0.90)	0.71 ± 0.04 (0.64–0.82)	0.71 ± 0.03 (0.63–0.77)	0.71 ± 0.05 (0.64–0.82)	0.70 ± 0.04 (0.63–0.77)	0.73 ± 0.05 (0.65–0.90)
Cerebellum left	0.59 ± 0.06 (0.48–0.74)	0.59 ± 0.06 (0.48–0.74)	0.59 ± 0.06 (0.48–0.68)	0.60 ± 0.06 (0.49–0.74)	0.59 ± 0.05 (0.49–0.67)	0.58 ± 0.07 (0.48–0.69)	0.59 ± 0.05 (0.49–0.65)
Cerebellum right	0.59 ± 0.07 (0.34–0.74)	0.60 ± 0.07 (0.35–0.73)	0.59 ± 0.08 (0.34–0.74)	0.60 ± 0.06 (0.50–0.71)	0.60 ± 0.09 (0.34–0.74)	0.59 ± 0.08 (0.45–0.74)	0.59 ± 0.07 (0.35–0.72)
Deep gray matter							
Caudate nucleus, left	0.76 ± 0.07 (0.54–0.91)	0.78 ± 0.07 (0.61–0.88)	0.75 ± 0.07 (0.54–0.91)	0.76 ± 0.09 (0.54–0.88)	0.77 ± 0.06 (0.63–0.88)	0.76 ± 0.08 (0.61–0.91)	0.76 ± 0.07 (0.65–0.87)
Caudate nucleus, right	0.76 ± 0.07 (0.62–0.93)	0.77 ± 0.07 (0.62–0.92)	0.76 ± 0.07 (0.63–0.93)	0.75 ± 0.07 (0.63–0.88)	0.75 ± 0.05 (0.67–0.88)	0.78 ± 0.06 (0.69–0.92)	0.77 ± 0.09 (0.62–0.93)
Putamen, left	0.75 ± 0.06 (0.63–0.89)	0.74 ± 0.06 (0.63–0.89)	0.75 ± 0.06 (0.66–0.89)	0.73 ± 0.05 (0.66–0.86)	0.74 ± 0.07 (0.63–0.89)	0.75 ± 0.05 (0.70–0.89)	0.77 ± 0.06 (0.65–0.88)
Putamen, right	0.74 ± 0.06 (0.62–0.90)	0.74 ± 0.06 (0.64–0.90)	0.74 ± 0.06 (0.62–0.88)	0.73 ± 0.05 (0.62–0.82)	0.74 ± 0.05 (0.64–0.86)	0.73 ± 0.05 (0.65–0.88)	0.76 ± 0.07 (0.64–0.90)
Thalamus, left	0.73 ± 0.03 (0.66–0.81)	0.73 ± 0.03 (0.66–0.81)	0.74 ± 0.04 (0.68–0.82)	0.73 ± 0.02 (0.68–0.77)	0.73 ± 0.03 (0.68–0.78)	0.73 ± 0.03 (0.68–0.78)	0.76 ± 0.05 (0.66–0.81)
Thalamus, right	0.73 ± 0.03 (0.67–0.82)	0.73 ± 0.03 (0.67–0.82)	0.74 ± 0.03 (0.68–0.81)	0.73 ± 0.02 (0.69–0.76)	0.72 ± 0.03 (0.68–0.78)	0.73 ± 0.03 (0.68–0.77)	0.76 ± 0.05 (0.67–0.82)
Other structures							
Internal capsule, left	0.51 ± 0.07 (0.32–0.64)	0.51 ± 0.07 (0.32–0.64)	0.52 ± 0.06 (0.36–0.62)	0.52 ± 0.06 (0.41–0.64)	0.50 ± 0.08 (0.32–0.62)	0.51 ± 0.07 (0.36–0.62)	0.53 ± 0.06 (0.39–0.63)
Internal capsule, right	0.52 ± 0.07 (0.34–0.63)	0.51 ± 0.07 (0.34–0.63)	0.52 ± 0.06 (0.36–0.62)	0.52 ± 0.06 (0.41–0.63)	0.50 ± 0.08 (0.34–0.62)	0.51 ± 0.07 (0.35–0.61)	0.53 ± 0.06 (0.38–0.63)
Pons, left	0.61 ± 0.07 (0.45–0.76)	0.61 ± 0.08 (0.45–0.76)	0.60 ± 0.07 (0.46–0.75)	0.62 ± 0.08 (0.46–0.75)	0.59 ± 0.07 (0.46–0.76)	0.62 ± 0.07 (0.51–0.76)	0.61 ± 0.08 (.45–0.73)
Pons, right	0.60 ± 0.07 (0.40–0.78)	0.59 ± 0.08 (0.40–0.78)	0.60 ± 0.07 (0.46–0.76)	0.61 ± 0.08 (0.46–0.76)	0.56 ± 0.06 (0.43–0.65)	0.62 ± 0.06 (0.51–0.75)	0.59 ± 0.07 (0.40–0.78)
Ventricle, frontal horn left	2.73 ± 0.27 (1.93–3.49)	2.72 ± 0.26 (2.67–3.26)	2.74 ± 0.29 (1.93–3.49)	2.57 ± 0.29 (1.93–2.99)	2.67 ± 0.23 (2.12–2.99)	2.78 ± 0.25 (0.25–3.17)	2.91 ± 0.21 (2.47–3.49)
Ventricle, frontal horn right	2.74 ± 0.27 (2.03–3.46)	2.73 ± 0.25 (2.16–3.16)	2.75 ± 0.29 (2.03–3.46)	2.57 ± 0.28 (2.03–3.05)	2.69 ± 0.23 (2.10–3.00)	2.79 ± 0.25 (2.27–3.16)	2.92 ± 0.21 (2.42–3.46)
Ventricle, middle part left	3.02 ± 0.16 (2.62–3.33)	2.99 ± 0.15 (2.66–3.31)	3.05 ± 0.17 (2.62–3.33)	2.94 ± 0.16 (2.62–3.26)	2.98 ± 0.15 (2.66–3.17)	3.05 ± 0.15 (2.72–3.31)	3.12 ± 0.13 (2.85–3.33)
Ventricle, middle part right	3.02 ± 0.16 (2.65–3.38)	3.00 ± 0.14 (2.67–3.26)	3.05 ± 0.18 (2.65–3.38)	2.95 ± 0.16 (2.65–3.25)	3.00 ± 0.15 (2.77–3.26)	3.03 ± 0.15 (2.66–3.32)	3.11 ± 0.14 (2.86–3.38)
Ventricle, posterior horn left	2.84 ± 0.35 (1.73–3.05)	2.87 ± 0.30 (2.05–3.35)	2.80 ± 0.40 (1.73–3.41)	2.82 ± 0.30 (2.36–3.25)	2.68 ± 0.37 (1.73–3.32)	2.82 ± 0.38 (1.84–3.35)	3.02 ± 0.30 (2.05–3.41)
Ventricle, posterior horn right	2.83 ± 0.35 (1.80–3.39)	2.85 ± 0.29 (2.22–3.38)	2.81 ± 0.40 (1.80–3.39)	2.81 ± 0.29 (2.35–3.26)	2.68 ± 0.37 (1.80–3.25)	2.83 ± 2.83 (1.83–3.38)	2.23 ± 0.26 (2.23–3.39)

Note.—Data are the means ± SDs. Data in parentheses are ranges.

TABLE 2: Mean ADC_{av} values for gray matter from all the cerebral lobes compared with mean ADC_{av} values for white matter

ROI	ADC_{av} ($\times 10^{-3}$ mm^2/s)						
	All (n = 80)	Men (n = 40)	Women (n = 40)	Age Group 1, 20–34 years (n = 20)	Age Group 2, 35–49 years (n = 20)	Age Group 3, 50–64 years (n = 20)	Age Group 4, 65–85 years (n = 20)
Gray matter	0.89 ± 0.04 (0.78–1.09)	0.90 ± 0.03 (0.84–0.96)	0.89 ± 0.05 (0.78–1.09)	0.90 ± 0.04 (0.84–0.96)	0.89 ± 0.04 (0.78–0.94)	0.90 ± 0.06 (0.81–1.09)	0.89 ± 0.03 (0.85–0.96)
White matter	0.70 ± 0.03 (0.62–0.79)	0.70 ± 0.03 (0.62–0.79)	0.71 ± 0.03 (0.66–0.79)	0.70 ± 0.02 (0.67–0.73)	0.70 ± 0.04 (0.65–0.79)	0.70 ± 0.03 (0.66–0.75)	0.71 ± 0.04 (0.62–0.79)
Basal ganglia	0.75 ± 0.03 (0.64–0.83)	0.75 ± 0.03 (0.69–0.83)	0.75 ± 0.04 (0.64–0.83)	0.74 ± 0.03 (0.64–0.80)	0.74 ± 0.02 (0.69–0.78)	0.75 ± 0.03 (0.69–0.81)	0.76 ± 0.04 (0.70–0.83)
Thalamus	0.73 ± 0.03 (0.67–0.82)	0.73 ± 0.03 (0.67–0.82)	0.74 ± 0.03 (0.68–0.81)	0.73 ± 0.02 (0.68–0.77)	0.72 ± 0.03 (0.68–0.78)	0.73 ± 0.03 (0.68–0.77)	0.76 ± 0.05 (0.67–0.82)

Note.—Data are the means ± SDs. Data in parentheses are ranges. Values in eight gray matter and eight white matter ROIs were compared.

mm^2/s) in the cortical gray matter, 0.70 ± 0.03 mm^2/s (range, 0.62–0.79 × 10^{-3} mm^2/s) in the white matter, (0.75 ± 0.03) × 10^{-3} mm^2/s (range, 0.64–0.83 × 10^{-3} mm^2/s) in the basal ganglia, and (0.73 ± 0.03) × 10^{-3} mm^2/s (range, 0.67–0.82 × 10^{-3} mm^2/s) in the thalamus. The regional ADC_{av} values are presented in Tables 1 and 2.

The mean cortical gray matter ADC_{av} value was significantly higher than the mean white matter value in all subjects ($P < .001$), in men ($P < .001$), in women ($P < .001$), and in all age groups ($P < .001$). ADC_{av} values in the basal ganglia and thalamus were higher than those in the white matter ($P < .001$), but they were lower than cortical gray matter values ($P < .001$) (Table 2). ADC_{av} values in the white matter in the various regions of the brain did not differ significantly. No statistically significant differences were found between the various cortical regions. The range of ADC_{av} values within each ROI was fairly large in all groups (Table 1). However, in every region and age group, the SDs of the ADC_{av} values were small.

In both lateral ventricles, the ADC_{av} values increased with age ($P < .001$). The homogeneity of the variances was normal in all the brain regions except the two thalami ($P < .002$ for the left and $P < .001$ for the right), where the ADC_{av} values in age group 4 were significantly higher than those of the other age groups. No other statistically significant age-related changes in the ADC_{av} values were noted. Differences in ADC_{av} values between the hemispheres were found only in the cerebellar gray matter; the left hemisphere had a higher ADC_{av} value than that of the right ($P < .02$). No differences were observed between the ADC_{av} values in the men and those of the women.

Discussion

We report absolute ADC_{av} values for the various regions of the human brain in a large representative adult population involving patients of both sexes with a wide age range. The study population was homogeneous; all subjects were white, and only two subjects were not Finnish. To our knowledge, no reports of normal ADC values in the brain in ethnically diverse populations exist, and whether our results can be directly extrapolated to people of different races requires further studies in such populations. Because the macro- and microstructural properties of the human brain are identical in people of various races, we believe that our results will prove to be valid for other populations as well.

The ADC_{av} values in the cerebral cortex were consistently higher than those of the white matter; this finding supports the results of previous studies (12, 15, 21, 22). This difference is partly due to the structural and functional differences between the cortex and the white matter (21). The cortex has higher water content and substantially higher blood flow compared with that of the white matter (23); both contribute to the ADC_{av} value. Furthermore, a partial volume effect of the CSF adjacent to the cortex may

increase the ADC_{av} values in the cortex (21, 22). In this study, the small variation among the ADC_{av} values within a cortical ROI indicated that CSF contamination was avoided. As expected, the ADC_{av} values in the CSF were more than twice as high as the gray matter values and almost three times as high as the ADC_{av} values in the white matter, because water diffusion is much less restricted in the CSF than in the brain tissue. In previous reports, the ADC values in the gray matter were $0.8–1.1 \times 10^{-3}$ mm^2/s, and those in the white matter were $0.6–0.9 \times 10^{-3}$ mm^2/s (12, 22); these values are similar to our results. The ADC_{av} values in the basal ganglia and thalamus were between the values in the gray matter and white matter, probably because of their microstructural properties (23).

Cerebellar gray matter ADC_{av} values were higher in the left hemisphere than in the right hemisphere. In the cerebellum, avoiding some overlap between the gray matter ROIs and the white matter, and probably the CSF, is difficult, because the cerebellar cortex is thin and has extensive folia. This partial volume effect may explain the wide range of cerebellar ADC_{av} values and the differences between the hemispheres.

Generally, the ADC_{av} values in the various brain regions did not change with aging. However, an age-dependent increase in ADC_{av} values was observed in the lateral ventricles, and the ADC_{av} values in the thalami in age group 4 were significantly higher than in those of the other age groups. Whether the change in the thalami was due to structural or functional changes related to aging or mere statistical artifact remains to be shown. The change in the ADC_{av} values in the lateral ventricles is possibly due to lower compliance in the aging brain and age-related enlargement of the ventricles, which allows more pulsatile movement of the CSF (24). This movement is likely to increase the turbulence of CSF flow (25), with a resultant increase in the measured diffusion (24). Gideon et al (15), in their study of 17 volunteers, found small age-related changes in the white matter but not in the gray matter. Other studies of ADC values in the healthy human brain have included only a few young subjects, or the total number of volunteers ranged between four and 15 (12, 16–18).

Absolute ADC values may be used to identify the ischemic tissue precisely (26), but their use requires a normal reference value for each brain region. Among human DW studies, only a few have involved the use of quantitative measurements (27–29). Quantitative methods, with absolute ADC values for healthy and pathologic structures, are important when focal and diffuse abnormalities are suspected, because minor changes may be difficult to detect by visual inspection. In experimental studies, comparisons of the ADC value in a given pixel before and after ischemia and the difference in ADC values in the infarcted and intact hemispheres have been used to detect early ischemia-induced ADC changes (1, 30–32). In humans, imaging before stroke is not feasible, and use of the contralateral side to provide a reference value may have limitations because of the possible existence of earlier lesions. A considerable amount of experimental work has been devoted to defining abnormal pixels and distinguishing normal pixels from ischemic pixels (26, 33–35). In studies of acute stroke, ADC values in the hyperacute (<6 hours after onset) ischemic lesion were less than 0.63×10^{-3} mm^2/s (3, 36, 37). In this study, the mean ADC_{av} values were $(0.89 \pm 0.04) \times 10^{-3}$ mm^2/s (range, $0.78–1.09 \times 10^{-3}$ mm^2/s) in the cortical gray matter, $(0.70 \pm 0.03) \times 10^{-3}$ mm^2/s (range, $0.62–0.79 \times 10^{-3}$ mm^2/s) in the white matter, and $(0.75 \pm 0.03) \times 10^{-3}$ mm^2/s (range, $0.64–0.83 \times 10^{-3}$ mm^2/s) in the basal ganglia; these results support the findings in hyperacute stroke studies. However, we identified some pixels with very low ADC_{av} values; the lowest was 0.32×10^{-3} mm^2/s, although most of the regional ADC_{av} values were within a narrow range, and the calculated SDs were small. The rare pixels with surprisingly low ADC_{av} values were randomly situated, and they may simply reflect blood vessels or technical errors. Because the ROIs were fairly large, these abnormal ADC_{av} values did not affect the results.

ADC values alone are not site specific. As can be seen from the white matter ADC_{av} values, no differences were found among the various brain regions. The same applies to the various cortical gray matter regions. Recent groups have indicated that knowledge of diffusion anisotropy can substantially improve the estimate for the anatomic location in question (38). In general, in the cerebral peduncles and internal capsule, the degree of diffusion anisotropy is high, whereas in the gray matter, diffusion is relatively isotropic (38–40). In the present study, the effects of anisotropy were overcome by using a rotationally invariant measure of diffusion (12).

Conclusion

In the present study, 80 healthy adult volunteers of both sexes with a wide age range were examined with spin-echo echo-planar DW imaging to establish reference normal average ADC_{av} values in the various regions of the brain. With the exception of the lateral ventricles, the ADC_{av} values were not affected by aging. The left and right hemispheres had similar ADC_{av} values, and no sex difference was observed. In normal brain, the ADC_{av} values in both gray matter and white matter were within a relatively narrow range. ADC_{av} values beyond these boundaries may indicate disease, and thus, DW imaging may be useful for tissue characterization. Our data are representative, and our findings can be used for reference in future studies and in clinical settings.

Acknowledgment

We thank Dr Fuhai Li for his critical review of the manuscript.

References

1. Li F, Han SS, Tatlisumak T, et al. **A new method to improve in-bore middle cerebral artery occlusion in rats: demonstration with diffusion- and perfusion-weighted imaging.** *Stroke* 1998;29:1715–1720
2. Li F, Han SS, Tatlisumak T, et al. **Reversal of acute apparent diffusion coefficient abnormalities and delayed neuronal death following transient focal cerebral ischemia in rats.** *Ann Neurol* 1999;46:333–342
3. Warach S, Gaa J, Siewert B, Wielopolski P, Edelman RR. **Acute human stroke studied by whole brain echo planar diffusion-weighted magnetic resonance imaging.** *Ann Neurol* 1995;37:231–241
4. Gonzalez RG, Schaefer PW, Buonanno FS, et al. **Diffusion-weighted MR imaging: diagnostic accuracy in patients imaged within 6 hours of stroke symptom onset.** *Radiology* 1999;210:155–162
5. Helpern JA, Huang N. **Diffusion-weighted imaging in epilepsy.** *Magn Reson Imaging* 1995;13:1227–1231
6. Hanuy H, Sakurai H, Iwamoto T, Takasaki M, Shindo H, Abe K. **Diffusion-weighted MR imaging of the hippocampus and temporal white matter in Alzheimer's disease.** *J Neurol Sci* 1998;156:195–200
7. Tievsky AL, Ptak T, Farkas J. **Investigation of apparent diffusion coefficient and diffusion tensor anisotropy in acute and chronic multiple sclerosis lesions.** *AJNR Am J Neuroradiol* 1999;20:1491–1499
8. Cercignani M, Iannucci G, Rocca MA, Comi G, Horsfield MA, Filippi M. **Pathologic damage in MS assessed by diffusion-weighted and magnetization transfer MRI.** *Neurology* 2000;54:1139–1144
9. Adachi M, Hosoya T, Haku T, Yamaguchi K, Kawanami T. **Evaluation of the substantia nigra in patients with Parkinsonian syndrome accomplished using multishot diffusion-weighted MR imaging.** *AJNR Am J Neuroradiol* 1999;20:1500–1506
10. Le Bihan D, Breton E, Lallemand D, Grenier P, Canabis E, Laval-Jeantet M. **MR imaging of intravoxel incoherent motions: application to diffusion and perfusion in neurological disorders.** *Radiology* 1986;161:401–407
11. Sakuma H, Nomura Y, Takeda K, et al. **Adult and neonatal human brain: diffusional anisotropy and myelination with diffusion-weighted MR imaging.** *Radiology* 1991;180:229–233
12. Ulug AM, Beauchamp N Jr, Bryan RN, van Zijl PCM. **Absolute quantitation of diffusion constants in human stroke.** *Stroke* 1997;28:483–490
13. Xing D, Papadakis NG, Huang CL, Lee VM, Carpenter TA, Hall LD. **Optimized diffusion-weighting for measurements of apparent diffusion coefficient (ADC) in human brain.** *Magn Reson Imaging* 1997;15:771–784
14. Burdette JH, Elster AD, Ricci PE. **Calculation of apparent diffusion coefficients (ADCs) in brain using two-point and six-point methods.** *J Comput Assist Tomogr* 1998;22:792–794
15. Gideon P, Thomsen C, Henriksen O. **Increased self-diffusion of brain water in normal aging.** *J Magn Reson Imaging* 1994;4:185–188
16. Tanner SF, Ramenghi LA, Ridgway JP, et al. **Quantitative comparison of intrabrain diffusion in adults and preterm and term neonates and infants.** *AJR Am J Roentgenol* 2000;174:1643–1649
17. Harada K, Fujita N, Sakurai K, Akai Y, Fujii K, Kozuka T. **Diffusion imaging of the human brain: a new pulse sequence application for a 1.5-T standard MR system.** *AJNR Am J Neuroradiol* 1991;12:1143–1148
18. van Everdingen K, van der Grond J, Kappelle LJ, Ramos LM, Mali WP. **Diffusion-weighted magnetic resonance imaging in acute stroke.** *Stroke* 1998;29:1783–1790
19. Shellock FG, Morisoli S, Kanal E. **MR procedures and biomedical implants, materials, and devices: 1993 update.** *Radiology* 1993;189:587–599
20. Salonen O, Autti T, Raininko R, Ylikoski A, Erkinjuntti T. **MRI of the brain in neurologically healthy middle-aged and elderly individuals.** *Neuroradiology* 1997;39:537–545
21. Le Bihan D, Turner R, Douek P, Patronas N. **Diffusion MR imaging: clinical applications.** *AJR Am J Roentgenol* 1992;159:591–599
22. Baird AE, Warach S. **Magnetic resonance imaging of acute stroke.** *J Cereb Blood Flow Metab* 1998;18:583–609
23. de Groot J, Chusid JG. *Correlative Neuroanatomy.* Stamford, Conn: Appleton & Lange; 1991;319
24. Bakshi R, Caruthers SD, Janardhan V, Wasay M. **Intraventricular CSF pulsation artifact on fast fluid-attenuated inversion-recovery MR images: analysis of 100 consecutive normal studies.** *AJNR Am J Neuroradiol* 2000;21:503–508
25. Sherman JL, Citrin CM, Gangarosa RE, Bowen BJ. **The MR appearance of CSF flow in patients with ventriculomegaly.** *AJR Am J Roentgenol* 1987;148:193–199
26. Dardzinski BJ, Sotak CH, Fisher M, Hasegawa Y, Li L, Minematsu K. **Apparent diffusion coefficient mapping of experimental focal cerebral ischemia using diffusion-weighted echo-planar imaging.** *Magn Reson Med* 1993;1994:318–325
27. Brockstedt S, Thomsen C, Wirestam R, Holtas S, Stahlberg F. **Quantitative diffusion coefficient maps using fast spin-echo MRI.** *Magn Reson Imaging* 1998;16:877–886
28. Chien D, Buxton RB, Kwong KK, Brady TJ, Rosen BR. **MR diffusion imaging of human brain.** *J Comp Assist Tomogr* 1990;14:514–520
29. Pierpaoli C, Jezzard P, Basser PJ, Barnett A, Di Chiro G. **Diffusion tensor MR imaging of the human brain.** *Radiology* 1996;201:637–648
30. Mintorovitch J, Moseley ME, Chileuitt L, Shimizu H, Cohen Y, Weinstein PR. **Comparison of diffusion- and T2-weighted MRI for the early detection of cerebral ischemia and reperfusion in rats.** *Magn Reson Med* 1991;18:39–50
31. Roussel SA, van Bruggen N, King MD, Houseman J, Williams SR, Gadian DG. **Monitoring the initial expansion of focal ischemic changes by diffusion-weighted MRI using a remote controlled method of occlusion.** *NMR Biomed* 1994;7:21–28
32. Davis D, Ulatowski J, Eleff S, et al. **Rapid monitoring of changes in water diffusion coefficient during reversible ischemia in cat and rat brain.** *Magn Reson Med* 1994;31:454–460
33. Hoehn-Berlage M, Norris DG, Kohno K, Mies G, Leibfritz D, Hossmann KA. **Evolution of regional changes in apparent diffusion coefficient during focal ischemia of rat brain: the relationship of quantitative diffusion NMR imaging to reduction in cerebral blood flow and metabolic disturbances.** *J Cereb Blood Flow Metab* 1995;15:1002–1011
34. Takano K, Latour LL, Formato JE, et al. **The role of spreading depression in focal ischemia evaluated by diffusion mapping.** *Ann Neurol* 1996;39:308–318
35. Takano K, Tatlisumak T, Formato JE, et al. **A glycine site antagonist attenuates infarct size in experimental focal ischemia: postmortem and diffusion mapping studies.** *Stroke* 1997;28:1255–1263
36. Marks MP, de Crespigny A, Lentz D, Enzmann DR, Albers GW, Moseley ME. **Acute and chronic stroke: navigated spin-echo diffusion-weighted MR imaging.** *Radiology* 1996;199:403–408
37. Nagesh V, Welch KM, Windham JP, et al. **Time course of ADCw changes in ischemic stroke: beyond the human eye!** *Stroke* 1998;29:1778–1782
38. Shimony JS, McKinstry RC, Akbudak E, et al. **Quantitative diffusion-tensor anisotropy brain MR imaging: normative human data and anatomic analysis.** *Radiology* 1999;212:770–784
39. Sorensen AG, Wu O, Copen WA, et al. **Human acute cerebral ischemia: detection of changes in water diffusion anisotropy by using MR imaging.** *Radiology* 1999;212:785–792
40. Conturo TE, Lori NF, Cull TS, et al. **Tracking neuronal fiber pathways in the living human brain.** *PNAS* 1999;96:10422–10427